

Review

# Recent Progress in Biomass-Derived Carbon Materials for Li-Ion and Na-Ion Batteries—A Review

Palanivel Molaiyan <sup>1</sup>, Glaydson Simões Dos Reis <sup>2,\*</sup>, Diwakar Karupiah <sup>3</sup>, Chandrasekar M. Subramaniyam <sup>4</sup>, Flaviano García-Alvarado <sup>4</sup> and Ulla Lassi <sup>1,5</sup>

<sup>1</sup> Research Unit of Sustainable Chemistry, University of Oulu, FI-90570 Oulu, Finland

<sup>2</sup> Department of Forest Biomaterials and Technology, Swedish University of Agricultural Sciences, Biomass Technology Centre, SE-901 83 Umeå, Sweden

<sup>3</sup> Department of Mechanical Engineering and Applied Mechanics, University of Pennsylvania, Philadelphia, PA 19104, USA

<sup>4</sup> Chemistry and Biochemistry Departamento, Facultad de Farmacia, Universidad San Pablo-CEU, CEU Universities, Urbanización Montepríncipe, Boadilla del Monte, 28668 Madrid, Spain

<sup>5</sup> Kokkola University Consortium Chydenius, University of Jyväskylä, FI-67100 Kokkola, Finland

\* Correspondence: glaydson.simoos.dos.reis@slu.se

**Abstract:** Batteries are the backbones of the sustainable energy transition for stationary off-grid, portable electronic devices, and plug-in electric vehicle applications. Both lithium-ion batteries (LIBs) and sodium-ion batteries (NIBs), most commonly rely on carbon-based anode materials and are usually derived from non-renewable sources such as fossil deposits. Biomass-derived carbon materials are extensively researched as efficient and sustainable anode candidates for LIBs and NIBs. The main purpose of this perspective is to brief the use of biomass residues for the preparation of carbon anodes for LIBs and NIBs annexed to the biomass-derived carbon physicochemical structures and their aligned electrochemical properties. In addition, an outlook and some challenges faced in this promising area of research is presented. This review enlightens the readers with valuable insights and a reasonable understanding of issues and challenges faced in the preparation, physicochemical properties, and application of biomass-derived carbon materials as anode candidates for LIBs and NIBs.

**Keywords:** biomass; carbon materials; lithium-ion batteries; sodium-ion batteries; anode materials



**Citation:** Molaiyan, P.; Dos Reis, G.S.; Karupiah, D.; Subramaniyam, C.M.; García-Alvarado, F.; Lassi, U. Recent Progress in Biomass-Derived Carbon Materials for Li-Ion and Na-Ion Batteries—A Review. *Batteries* **2023**, *9*, 116. <https://doi.org/10.3390/batteries9020116>

Academic Editors: Pascal Venet, Karim Zaghib and Seung-Wan Song

Received: 18 December 2022

Revised: 2 February 2023

Accepted: 4 February 2023

Published: 7 February 2023



**Copyright:** © 2023 by the authors. Licensee MDPI, Basel, Switzerland. This article is an open access article distributed under the terms and conditions of the Creative Commons Attribution (CC BY) license (<https://creativecommons.org/licenses/by/4.0/>).

## 1. Introduction

With the earth's human population growing to 8 billion, the energy demand is increasing at alarming rates. The depletion of global natural resources and the environmental crisis, opt for the development of low-cost renewable, and sustainable high-energy and power-density energy storage systems, such as batteries as these natural sources are intermittent. Due to their high energy density and power output, outstanding safety, and long cycle life, lithium-ion battery (LIBs) is the most used technology revolutionizing the portable electronic world and is now being pursued to develop plug-in electric vehicles [1–4]. For example, the global grid-battery energy storage market has been forecast an annual growth rate of 23% or even more by 2030. However, lithium (Li) is a very limited resource in the earth's crust containing only 0.0017 wt.%, and their mining deposits are situated in politically unstable countries making them very expensive to cast as “white gold” [5].

Therefore, the focus is directed towards developing energy storage devices with earthly abundant and sustainable elements such as sodium-ion batteries (NIBs) that are believed to be the most suitable battery technology to replace LIBs, because of stationary applications such as wind energy storage. Sodium (Na) is cheaper and more abundant than Li, with an estimated 2.8 wt.% of total Na concentration in the earth's crust [6,7]. In addition, Na and Li have similar physical and chemical properties but differ in their energy density

due to their standard electrode potentials:  $-2.71$  V vs. SHE ( $\text{Na}^+/\text{Na}$ ) and  $-3.04$  V vs. SHE ( $\text{Li}^+/\text{Li}$ ) and different atomic radii [8]. However, NIBs have sluggish kinetics and lower energy/power density compared to LIBs which slows down their massive employment in mobile devices and electric vehicles; but allows NIBs to be employed in massive stationary storage applications (e.g., grid energy storage) where energy density and battery size are not critical factors [9,10].

One of the key parameters for efficient battery technologies (NIBs or LIBs) is the right development of sustainable and high-capacity anode materials. Nowadays, graphite (Gr) is the most common anode material for LIBs [11–13]. Carbon nanotubes and graphene appear as important anode materials as well [14,15]. However, these types of carbonaceous materials face serious drawbacks including high production costs, extremely complex large-scale fabrication, and/or non-sustainable routes/processes [16]. Then, it is highly necessary to develop novel, eco-friendly, cheap carbon-based functional materials with sustainable and scalable synthesis/fabrication processes [17]. Considering this statement, carbon anode materials from biomass resources have gathered huge interest due to their easy processing and handling, non-toxicity, and worldwide availability and abundance of biomass resources [18–22]. Also, biomass carbon materials can be easily turned into hierarchically porous structures to be employed in battery technologies due to their excellent cycling stability and rate performance. Figure 1 represents an exponential increase in the literature-reported related biomass anodes for LIBs and NIBs applications from 2012 to 2022.

The scientific society has responded to the request for sustainable bio-based electricity storage devices through a tenfold increase in scientific publications over the last decade [19,21,23]. To date, plenty of research has dealt with biomass-derived carbon anodes for batteries application [18–22]. Some main advantages of using bio-based carbon anodes for batteries can be simplified into some main characteristics such as (i) large interlayer spaces that provide excellent physical-mechanical stability during ion intercalation/deintercalation process [24]; (ii) different and large amounts of surface functionalities that boost the charge transfer [25]; (iii) high specific surface area (SSA), well developed pore structures with different nano-sizes, and good thermal stability, fast mass transports; (iv) the surface and structure of the bio-based carbons can be easily modified/tailored, in terms of its chemical structure and surface functionalities, e.g., by heteroatom doping (Nitrogen, Oxygen, Sulphur, etc) to boost the electrochemical performance (e.g., lifetime, capacity and safety) [26]; (v) wide availability/accessibility facilitate the developing of multiple carbon anodes using different types of biomass carbons and composites by simple synthesis methods [20–22].

To obtain high/performance and suitable anode materials for LIBs and NIBs, relevant biomass-carbon anode material properties—such as the porosity and pore structure, interlayer spacing, structural defects, and number and type functionalities—need to be tuned. By employing carbon anode materials from biomass, it is possible to simplify the process significantly and switch to renewable and eco-friendly feedstock. This review shows different strategies for the employment of biomass residues as sustainable and efficient precursors to fabricate carbon anodes for LIBs and NIBs. It mainly focuses on the relationship between the composition of biomass precursor and synthesis method to physicochemical properties of biomass-derived carbon nanostructure over their electrochemical performances in LIBs and NIBs. In addition, this report is of further interest to scientists who seek out novel, easy fabrication, and low-cost anode materials from different types of biomasses, which opens new avenues in the fabrication/development of next-generation sustainable and high-energy density batteries.

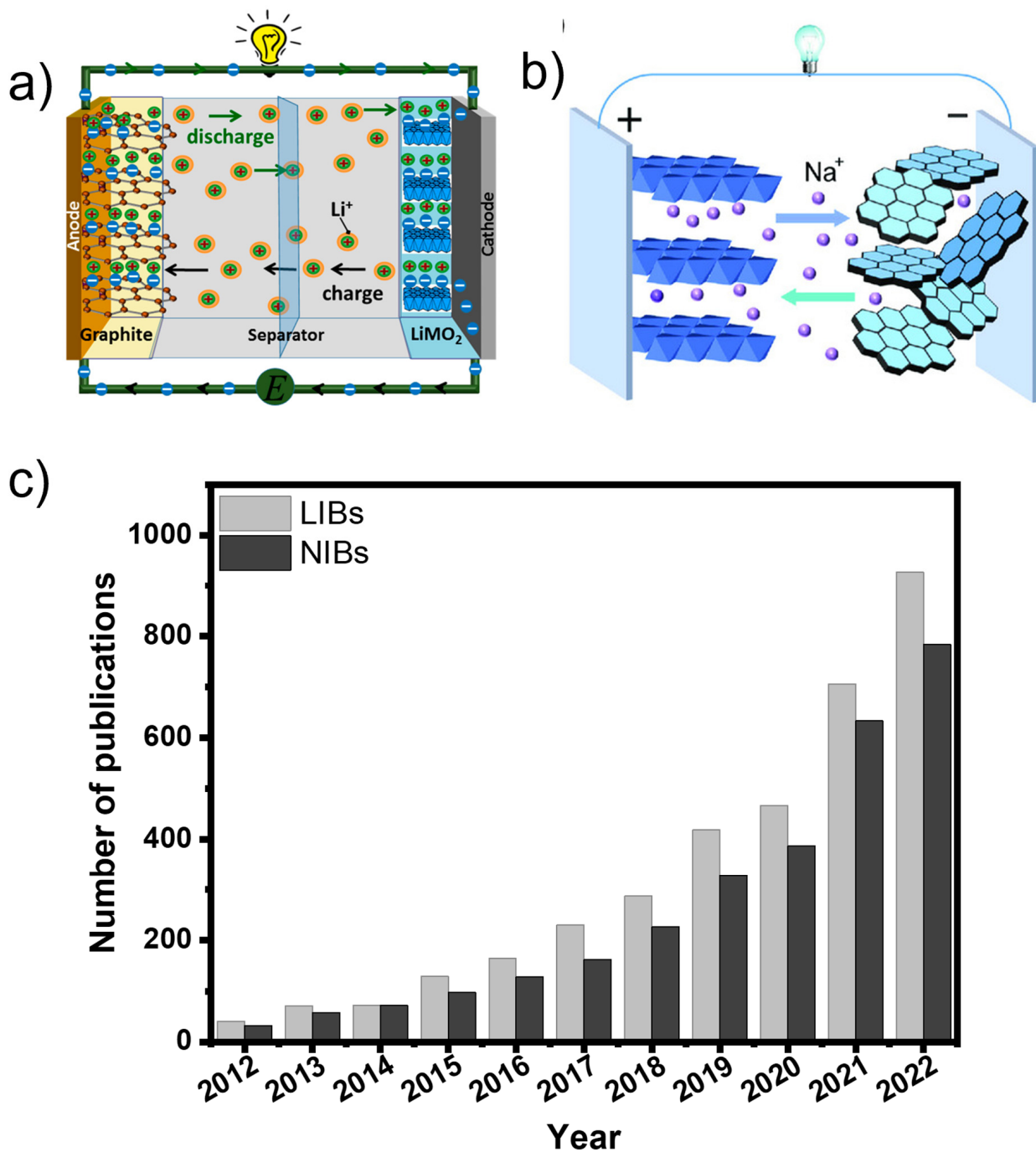


**Figure 1.** (a,b) A schematic and working principle of LIBs (Reproduced from [9] with permission from MDPI) and NIBs (Reproduced from [10] with permission from Wiley). (c) The number of published articles from 2012 to 2022 for “biomass anodes for lithium-ion battery” and “biomass anodes for sodium-ion battery” (Web Source: Science Direct).

## 2. Li-Ion Batteries (LIBs)

Lithium-ion batteries (LIBs) are the well-established and more dominating battery technology and are already the most widely used in our society. It has been an enabling technology for portable electronic devices and is revolutionizing the automotive industry [3,27]. To achieve a better energy transition, high energy density batteries are intensively researched worldwide, LIBs having emerged as one of the most promising energy storages [28]. LIBs are increasing in popularity despite rising prices and uncertainty around

sourcing component materials. However, due to the rising demand and unequal geographic distribution, Li and Gr are becoming ever-increasing strategic resources [17]. LIB uses  $\text{Li}_4\text{Ti}_5\text{O}_{12}$  (LTO) or Gr as the anode and lithium cobalt oxide (LCO), lithium iron phosphate (LFP), lithium manganese oxide (LMO), lithium nickel-manganese-cobalt (NMC), lithium nickel-cobalt-aluminum oxide (NCA) as cathode materials [28,29]. Almost 95% of the world's LIBs are produced in Asian countries like Japan, South Korea, China, and Taiwan. However, Gr has been used widely as anode materials for LIBs and could not meet the requirements due to the limitations in energy capacity and reliable operation. Alternatively, several anode materials have been widely investigated and tried to replace Gr, such as silicon, tin, and simple binary transition metal oxides [30–32], even Li metal for solid-state batteries, and especially, biomass-derived carbon materials with special morphologies and structures because these, generally, exhibit high specific capacity.

### 3. Sodium-Ion Batteries (NIBs)

Sodium-ion battery (NIB) is a type of rechargeable battery like the LIB but uses sodium ions ( $\text{Na}^+$ ) as the charge carrier. NIBs have several advantages over competing for battery technology, but furthermore, research and development are still needed to fully exploit them [33–35]. Several companies are developing commercially viable NIBs for different applications, but NIBs with high energy densities, excellent electrochemical performance, and high stability are not yet commercialized though a couple of companies have announced imminent productions (for example, CATL and BYD). If the cost of NIBs is further reduced, they will be favored for energy storage in grids, where battery weight is not important [35–38]. The NIBs are electrochemical energy storage devices like LIBs because both are working in the same principle (intercalation and deintercalation). Then the question is why we should concentrate on NIBs rather than LIBs, even though they have lower energy density [39–41]. LIBs materials, mainly Li, are not abundant in nature. However, researchers are looking for alternative batteries for electric vehicles to protect against energy crises and global warming. Once the demand for electric vehicles increases. It can automatically increase the demand for batteries. Hence, it should create a big problem in the supply chain process due to the deficiency of Li sources. It is noted that the solution to this Li shortage problem has been fulfilled by NIBs because of their abundant nature, low cost, etc. Therefore, the research on NIBs might capture more attention [42,43].

NIBs were originally developed in the early 1980s, approximately over the same time period as LIBs. During this time intercalation process of  $\text{TiS}_2$  could be tested for both LIBs and NIBs. In 1990, low-cost, moderate-capacity graphite anode was also tested for both battery chemistries. The LIBs battery shows a better output than NIBs. This was the reason for ignoring NIB. Then, development based on Na metal batteries is highly focused because of their energy density. These devices are only working at elevated temperatures (300 to 350 °C) for ensuring the liquid state Na (melting point 98 °C). Here, (sodium  $\beta$  alumina) solid-state electrolytes (" $\beta$ -alumina") were used as the ion transport medium. However, the poor power density, security issues, and more expansive implementation of the batteries again stop its development. Room temperature NIBs are widely recognized as the alternative candidates for LIBs [44]. NIB comprises of cathode, electrolyte, separator, and anode. The cathode should be reversibly accommodated  $\text{Na}^+$  at a voltage greater than 2 V vs.  $\text{Na}/\text{Na}^+$ . In oxide-based cathode compounds,  $\text{Na}^+$  occupies only octahedral or prismatic sites because the large size of  $\text{Na}^+$  exhibits less stability with four coordinates (tetrahedral) than Li-ion. On the other hand, polyanionic materials have octahedral interstitials in their structures. These cathodes look promising candidates for NIBs [42]. At room temperature, organic electrolytes have superior electrochemical properties for NIBs. This organic solvent is a mixture of propylene carbonate (PC), ethylene carbonate (EC), diethyl carbonate (DEC), and ethyl methyl carbonate (DMC) with sodium salt  $\text{NaPF}_6$ . It can have good ionic conductivity, chemical stability, and potential window. The successful anode must have a lower voltage (less than 2 V) and act as a good host for  $\text{Na}^+$  [42].

#### 4. Biomass-Derived Carbon Materials-Syntheses and Properties for LIBs and NIBs

As mentioned in the earlier, many carbon allotropes and textures like Gr, CNT, graphene etc, although, pronounced good electrochemical reversibility [45] but face critical challenges due to complex synthesis methods and high production costs and hence, tempering their large-scale production [45]. Thus, the preparation of carbon-based materials from sustainable resources such as biomasses is of great interest because biomass is a widespread worldwide, non-toxic and inexpensive resource. In addition, it can be easily processed into porous and rich in functionalities materials, which are good requirements for battery application. Carbon materials derived from biomass precursors can contain desired/suitable properties e.g., SSA, different pore structures (micro and meso pores), the high number of functional groups on its surfaces, adjustable hydrophilicity, and conductivity [19]. Thanks to all these properties, they can be successfully employed as anode materials for LIBs and NIBs [19].

Carbon materials are commonly classified into two main categories, graphitizable (soft carbons) and non-graphitizable (hard carbons). Soft carbons can be tuned into graphite while subjected to very high temperatures ( $>2000$  °C), while hard carbons are hardly graphitized even at 3000 °C. Figure 2 shows the basic structure of Gr, soft, and hard carbons. The type and composition of the carbon raw material strongly influence the graphitization degree of the carbon material. A high graphitization degree is facile achieved with aromatic precursors (coal tar and petroleum pitch) that easily form non-porous soft carbon materials [19]. On the other hand, carbon materials from biomass, which have much less aromatic structures, can provide well-developed porous and amorphous structures (hard carbons) [46]. Hard carbon is largely reported as an excellent candidate for NIBs but also a promising candidate for LIBs, thanks to its excellent cyclability and high physico-chemical stability [19]. However, unlike Gr, the most detailed electrochemical mechanism for LIBs using hard carbon remains unknown. Gr in LIBs form stable intercalated  $\text{LiC}_6$  that delivers a moderate theoretical intercalation capacity of  $372 \text{ mA h g}^{-1}$ , while its intercalation capacity for NIBs is far from satisfactory, delivering only  $35 \text{ mA h g}^{-1}$  for with  $\text{NaC}_{64}$ , thus graphitic structures are not desired for NIBs application. The literature reports that hard carbons can reach a very high LIBs specific capacity ( $\approx 1000 \text{ mA h g}^{-1}$ ), much higher than ( $\approx$ three times that of Gr anode) which is highly promising for very high energy density LIBs [47]. For NIBs, hard carbon can also have extraordinary performances. Tian et al. [48] prepared a composite of Phosphorus/hard carbon from a coconut shell by filling red phosphorus nanoparticles into the pores of the hard carbon. The composited hard carbon contained nearly half of its weight (wt.%) of P in its structure. When it is applied as an anode in NIBs. The material delivered an extremely high reversible capacity of  $2481 \text{ mA h g}^{-1}$  at  $50 \text{ mA g}^{-1}$  with a higher 89% initial Coulombic efficiency (ICE) and after 100 cycles, the material displayed a capacity of  $993 \text{ mA h g}^{-1}$  at  $0.5 \text{ A g}^{-1}$ , and keeping a ICE of 89%.

The literature shows that the properties of carbon materials are widely dependent on pyrolysis conditions, especially temperature. Figure 3 summarises the main features of the carbon materials versus pyrolysis temperature. These features play a huge role in electrochemical performances of carbon materials when employed as anodes for battery applications [19,47]. It is well known that other pyrolysis and preparation parameters such as type of biomass and its composition, pyrolysis time, used catalyst, heating rate, and reaction atmosphere, do influence the carbon material's final properties and that all these parameters act concomitantly [49].

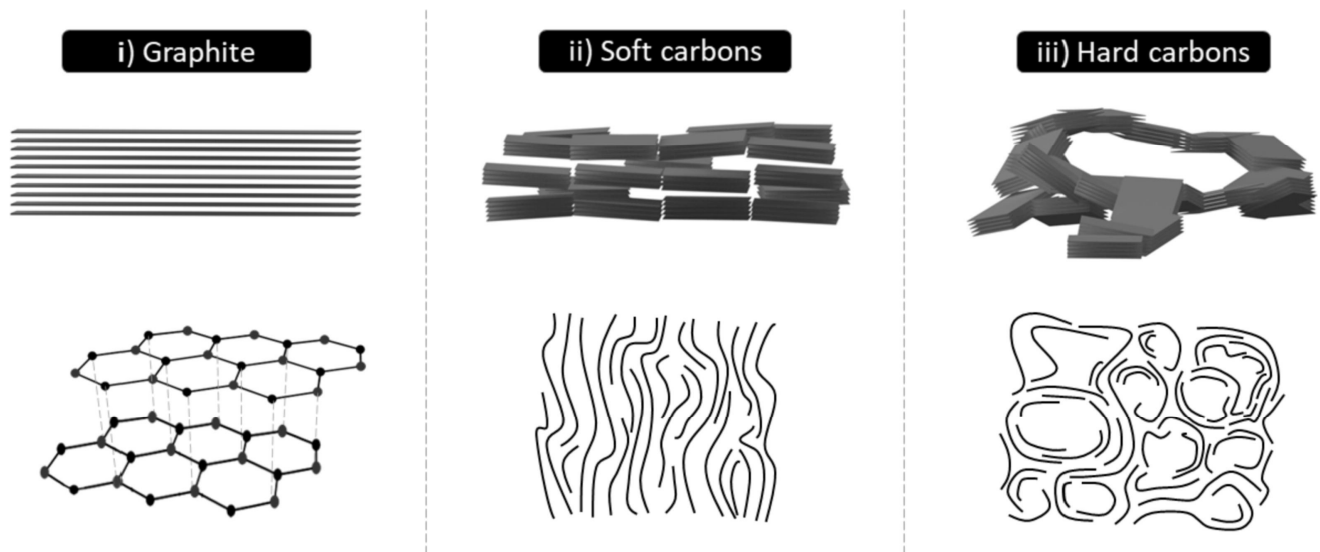


**Figure 2.** Schematic structures of Gr, soft carbon, and hard carbon. Reproduced from [19] with permission from Elsevier.

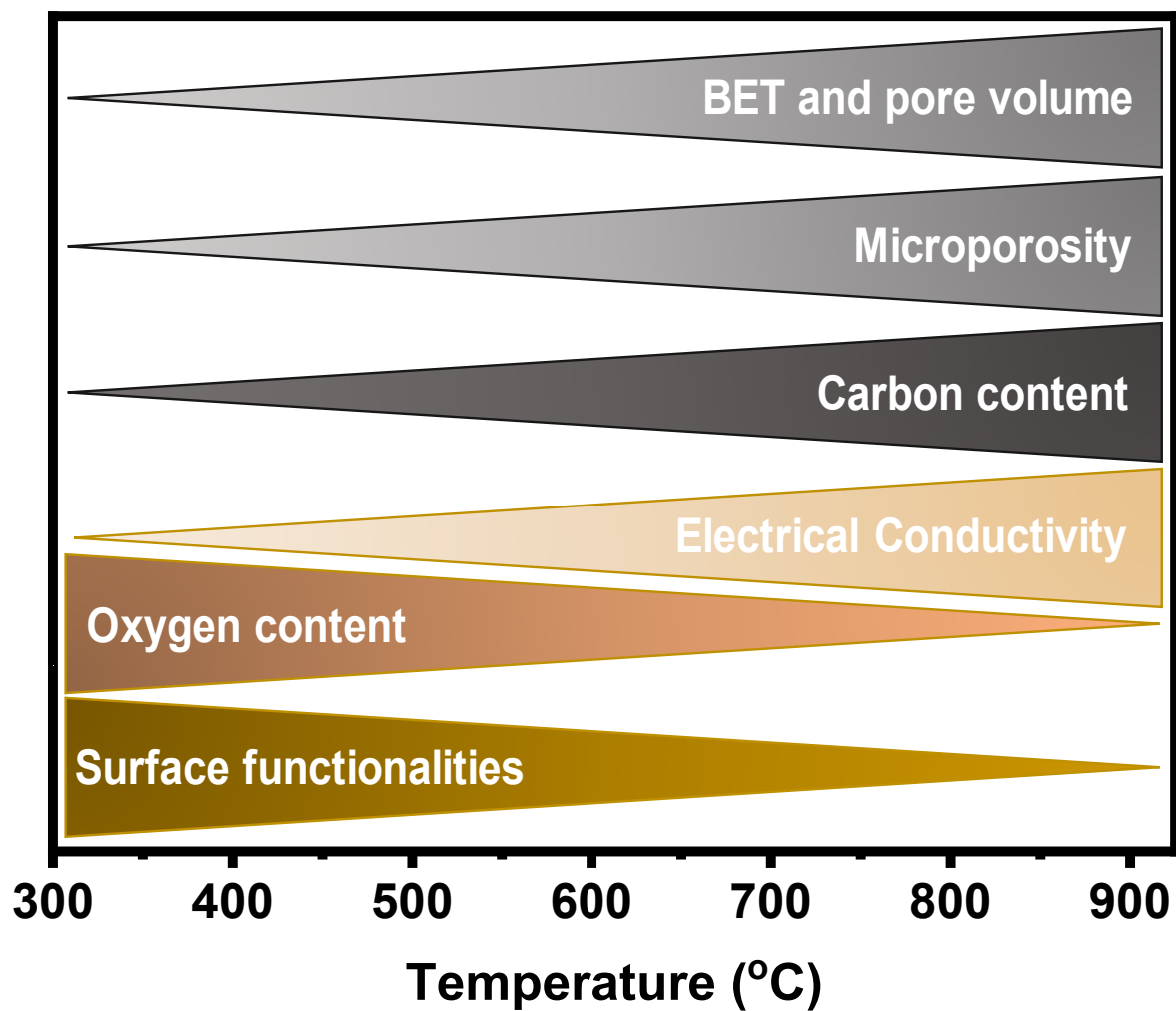


**Figure 3.** Variation in biochar properties with an increase in pyrolysis temperature conditions.

During the carbon material formation, the surface functionalities and oxygen contents tend to decrease with the increase of the pyrolysis temperature because O and H atoms are released into the gas phase due to the volatilization process of the biomass compounds and cracking of the residual char [49]. Carbon materials when used as anodes in batteries, surface functionalities, and oxygen content are very important features because they can also boost the batteries capacities and power densities. After all, the oxygen functionalities can drive uniform Li deposition without the formation of dendrites [50].

Zhao et al. [51] studied the presence of oxygen functionalities on mesoporous carbon anodes in NIBs and showed that that carboxylic acids ( $-C(=O)OH$ ), ketones ( $R_2C=O$ ), and lactones ( $-C(=O)-O-$ ) slightly reduced the intrinsic electronic conductivity of the carbons, while the presence of carboxylic anhydrides and quinones increased electronic conductivity. They reported that these groups and lactones have the best affinity toward  $Na^+$  adsorption. In another work, Sun et al. [52] synthesized carboxyl-rich carbon surface with up to 20.12 atomic wt.% oxygen content. They found that  $-COOH$  groups acted as active sites for  $Na^+$  capacitive adsorption by electrostatic interactions which boosted the NIB storage capacity. Wang et al. [53] corroborate that the oxygen functionalities such  $C=O$  and  $COOH$  improved the reversible charge capacity and ICE of the carbon anodes. Although surface functional groups (like  $-COOH$ ) have a beneficial effect on electrochemical performances, they can have negative affect because of the formation of thick solid-electrolyte-interface (SEI) layer which lead to the largely irreversible loss during the first cycles [54]. Ventosa et al. [55] reported that the irreversible charge loss of a LIB increased with higher amount of oxygen functionalities due to the formation of a thicker SEI layer. Therefore, the less O content and more C content is beneficial. The literature shows that oxygen-containing functional groups suffer huge reduction with the increasing of pyrolysis temperature [56].

Heteroatom doping is the most employed strategy to introduce functionalities on biomass-derived carbon surfaces [25,57,58]. The heteroatom doping induces electron density changes that alter the polarity of the carbon surface, promoting the formation of binding sites for molecules or ions, and making the surface catalytically active for different reactions including in batteries [57]. Among heteroatom doping nitrogen (N) is the most performed one [25,57,58]. N doping introduces high electronegativity and creates many defects within the carbonaceous matrix which can also increase the SSA [25]. Besides, N acts as an electron donor that gives more electrons to the delocalized carbon network, increasing the electronic conductivity and therefore, boost the  $Li^+$  and  $Na^+$  storage capabilities. Other common heteroatoms used for carbon material doping are sulfur (S), boron (B), fluorine (F), and phosphorus (P) and they are active in the same way as N doping by often being used to improve electrochemical performances of biomass-derived carbon anodes [57].

Among the properties presented in Figure 3, the electrical properties, and especially electrical conductivity (EC), is well-known to play a pivotal role in the performance of any anode material. The EC of porous carbons largely influences electrode electrochemical performances in energy storage device applications [19,59]. The EC is largely influenced by the pyrolysis condition and many reports show that the conductivity of the carbon materials increases with pyrolysis temperature [60–63]. The increase in the EC at higher temperatures may be explained by the chemical decomposition of the biomass turning it into a carbon structure with a high degree of  $sp^2$  structures [63]. In addition, at higher temperatures, graphitic crystallite structures appear within the carbon matrices, and at lower temperatures, these structures can be embedded within or between the amorphous carbons resulting in low EC values [63]. It is worthwhile to mention that doping the carbon materials with heteroatoms is an efficient technique to increase the EC [64]. The introduction of heteroatoms such as N, S, B, P, etc., into carbon materials, offer the possibility of tailoring not only their structural but also their electronic properties (Figure 4). Mousavi and Moradian [64] studied the effect of N and B doping on carbon materials EC properties and found that this is an efficient technique to boost it. They reported that the insertion of a heteroatom in the carbon structure leads to an increased electrical conductivity due to

electron excess in the delocalised  $\pi$ -system, creating structural defects in the carbon bonds and then changing the electronic configuration of the carbon materials [64,65].

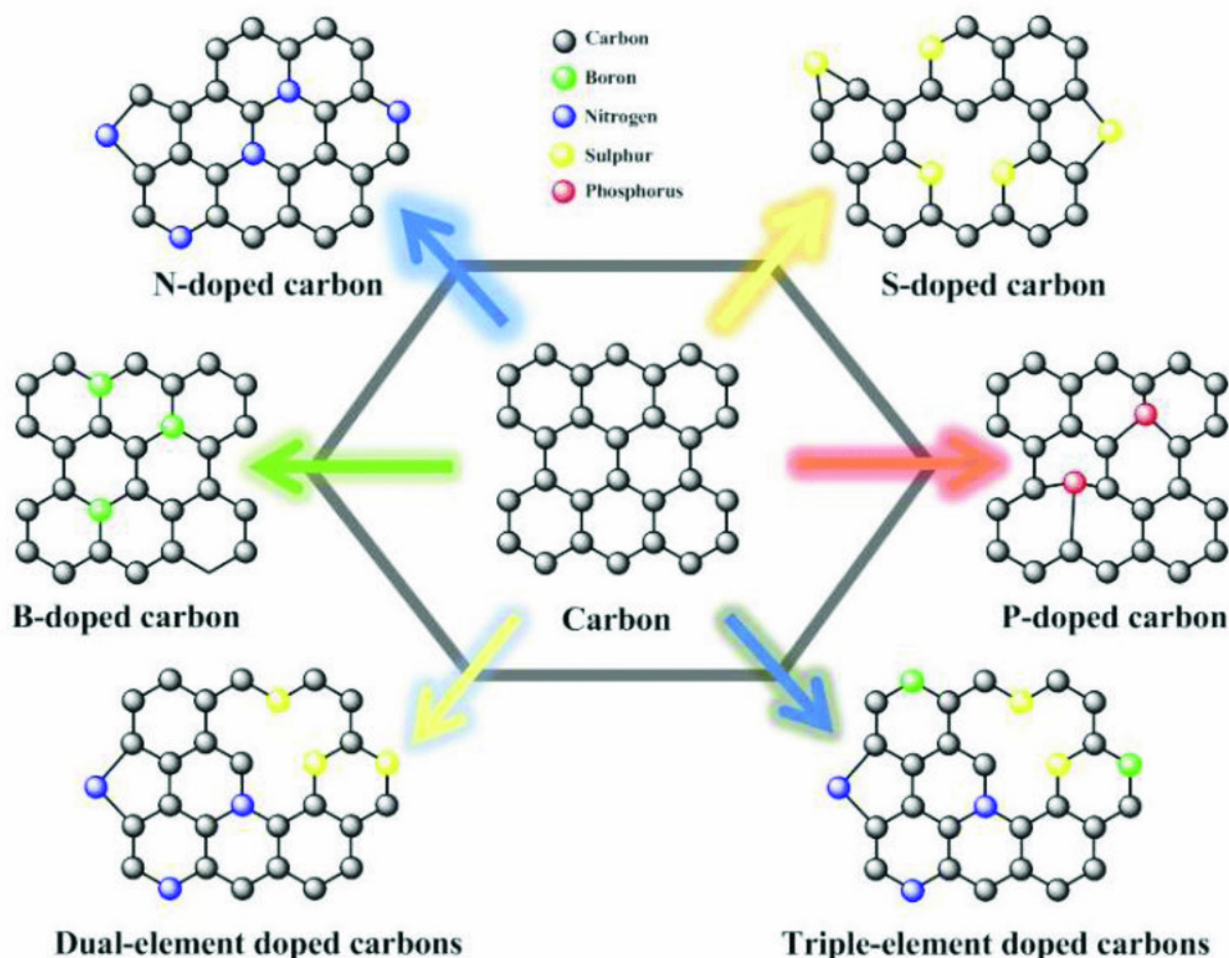


**Figure 4.** Scheme of various heteroatom-doped carbons. Reproduced from [57] with permission from Wiley.

Another heteroatom that is efficiently used for improving the anodes electrochemical properties is sulfur because it enhances the interlayer distance of carbon structure due to its larger covalent diameter, which reflects in an improvement of  $\text{Na}^+$  intercalation [66]. Sulfur creates  $\text{C-S}_x\text{-C}$  ( $x = 1, 2$ ) covalent bonds, which enhance the carbon anode electronegativity resulting in better values for the reversible storage of  $\text{Na}^+$  and improving its reversible capacity. Boron doping also enhances the lattice expansion which can be beneficial for  $\text{Na}^+$  storage but also  $\text{Li}^+$ . Doping the carbon materials with fluorine (fluor) is also extremely beneficial for both  $\text{Na}^+$  and  $\text{Li}^+$  storage, fluorine creates carbon materials with boosted electrical conductivities which improves the  $\text{Na}^+$  and  $\text{Li}^+$  adsorption [67]. Zhang et al. [64] prepared F-doped mesoporous carbon with 8.35 at % of fluor. The F-doped materials had its interlayer spacing enlarged to 0.402 nm, which is larger than the minimum required for  $\text{Na}^+$  ion insertion (0.37 nm) as predicted by theoretical calculations [68] that is highly beneficial for  $\text{Na}^+$  and  $\text{Li}^+$  insertion/de-insertion process.

One of the most important porous carbon properties is the specific surface area (SSA, in  $\text{m}^2 \text{g}^{-1}$ ) that often obeys the trend of increasing their values with the increase of pyrolysis temperature placing these pyrolysis parameters as the widely influential to obtain higher SSA values [69,70]. However, many reports show that the type of biomass source and chemical or physical treatments employed also play a huge influence on SSA and pore characteristics of the carbon materials. Guy et al. [69] statistically studied the effect of

three variables (temperature, pyrolysis time, and KOH ratio) on the SSA of activated carbon materials from tree wastes. The authors found that temperature had the most positive effect on SSA values among all three parameters. The same trend was reported by Bouchelta et al. [70] stating that the temperature largely affected the SSA and pore volume values of carbon materials from date pits. Other reports found out same positive trends between pyrolysis temperature and SSA [71].

For the efficient development of porous carbon materials, the activation step is crucial to obtain materials with high SSA values. The activation can be either physical and/or chemical that can take place during the pyrolysis in either a single or two-stage process. For chemical activation, the biomass must be mixed with chemicals and the most commonly used ones are  $\text{ZnCl}_2$ , KOH, NaOH,  $\text{H}_3\text{PO}_4$ ,  $\text{K}_2\text{CO}_3$ , and  $\text{FeCl}_3$ , etc. [72,73]. Each chemical provides carbon materials with different porous structures, and they can be deliberately used to obtain carbon materials with tailored/desired properties [72,73]. Glaydson Simões dos Reis et al. [72] studied the properties of carbon materials made with KOH and  $\text{ZnCl}_2$ . The materials were subjected to high pyrolysis temperatures (700 °C and 900 °C). The KOH carbon material displayed an SSA of  $1881 \text{ m}^2 \text{ g}^{-1}$  while the sample made with  $\text{ZnCl}_2$  exhibited an SSA of  $1294 \text{ m}^2 \text{ g}^{-1}$ . Although is abundant in the literature that the SSA increases with increasing temperature, it is known that at very high temperatures (>1000 °C), the SSA values tend to decrease because of shrinkage of the biochar's narrowing their pores leading to collapsing their meso/microporosity at such extremely high temperatures. In another work, Glaydson Simões dos Reis et al. [73] employed four different chemical treatments (KOH,  $\text{ZnCl}_2$ ,  $\text{ZnSO}_4$ , and  $\text{MgCl}_2$ ) for the preparation of carbon materials. It was reported that KOH produced a carbon with the highest SSA value ( $2209 \text{ m}^2 \text{ g}^{-1}$ ), followed by  $\text{ZnCl}_2$ ,  $\text{ZnSO}_4$ , and  $\text{MgCl}_2$  with respective SSA values of 1019, 446, and  $98 \text{ m}^2 \text{ g}^{-1}$ . In addition, the different chemical treatments influenced the oxygen and carbon contents, (86.6% of C and 10.5% of O), (94.7% of C and 4.4% of O), (95.6% of C and 3.0% of O), and (97.0% of C and 2.7% of O), for KOH,  $\text{ZnCl}_2$ ,  $\text{ZnSO}_4$ , and  $\text{MgCl}_2$ , respectively.

To summarize, easily tunable biomass-derived carbon materials appear to be the next generation of high-energy density anode candidates for LIBs and NIBs. To fit the properties of the biomass carbon anodes to LIBs and NIBs requirements, the synergic effects of combined factors previously discussed must be carefully evaluated during the synthesis of the carbon materials. Pyrolysis, activation, and heteroatom doping strategies must be properly understood and combined to achieve the optimal balance among the most important physicochemical/electrochemical parameters for high energy and power density biomass carbon anodes.

## 5. Biomass Carbon Anode for LIBs

Biomass-based hard carbon anodes avoid using critical Li, as in LTO and Gr. In addition, the LIB anodes produced with Gr, carry a large  $\text{CO}_2$  footprint and high costs [3,13]. Thus, especially, biomass-derived hard carbons have attracted attention as a sustainable source for high-performing rechargeable batteries anodes. Extensive research are been made for developing efficient and sustainable materials where many biomass wastes are employed as precursors for carbon-based anode materials for LIBs. Biomass carbon-derived materials have good and adaptable structural and functional properties, making them suitable for use as anodes for LIBs. In addition, using biomass residues (and not Gr) to produce efficient anodes would be both environmentally friendly and economically advantageous. Sisal fibers are a kind of low-cost and renewable biomass resource and offer excellent mechanical properties for LIBs. Xinliang Yu et al. [74] study the activated carbons to provide good cycling stability and capacity from the hydrothermal activation method derived from sisal fibers pyrolytic carbon as anode material for LIBs. The biomass carbons derived from sisal fibers reported the honeycomb structure like morphology and content of disordered carbon sheets. Celia Hernández-Rentero et al. [75] reported that environmentally sustainable anode material with irregular carbons from biomass from the cherry pit and activated by either KOH or  $\text{H}_3\text{PO}_4$  via the chemical method. The anode is

paired with  $\text{LiFePO}_4$  (LFP) cathode and delivered the specific capacity of  $160 \text{ mA h g}^{-1}$  and capacity retention of 95% for almost 200 cycles at C/3 rate. Dou et al. [76] synthesized porous carbons derived from jute fiber through  $\text{CuCl}_2$  activation and tested them as anodes for LIBs. The carbon materials were named according to the amount of  $\text{CuCl}_2$  JFC-0 (no  $\text{CuCl}_2$ ), JFC-6 (1:6 molar ratio of biomass:  $\text{CuCl}_2$ ), JFC-8 (ratio 1:8), and JFC-10 (1:10). Porous carbon with specific surface area (SSA) up to  $2043 \text{ m}^2 \text{ g}^{-1}$  were reported for JFC-8 and the specific capacity was delivered equal to  $580.4 \text{ mA h g}^{-1}$  at the current density of 0.2 C after 100 cycles, which is highest among all samples. The authors reported that this high capacity was due to the (a) high SSA area that increases the active electrode/electrolyte contact area, accelerating mass diffusion, (b) the presence of macropores that improves the transport of electrolyte and enhance the  $\text{Li}^+$  diffusion, (c) the high presence of micropores that acted as deep trap sites for  $\text{Li}^+$  storage and thus improving the capacity of  $\text{Li}^+$  storage, and the presence of mesopores provided ion-highways for ion transfer. These factors contributed to the high  $\text{Li}^+$  storage on the jute fiber carbon anode for LIBs. Table 1 represents the various biomass-derived anode materials (sisal fiber, banana peel, bagasse, portobello mushroom, coffee waste grounds, etc) and their performances for LIBs.

dos Reis et al. [77] produced activated biochars from wood wastes with different SSA and pore structures based on its chemical activation ( $\text{ZnCl}_2$ , Biochar-1) with SSA value  $1294 \text{ m}^2 \text{ g}^{-1}$  and content of mesopores (96.1%). Activation with KOH (Biochar-2) with higher SSA ( $1881 \text{ m}^2 \text{ g}^{-1}$ ) and lower content of mesopores (56.1%). When employed as anodes for LIBs, Biochar-1 exhibited much better electrochemical features compared to Biochar-2, with excellent rate capability and higher capacities of  $370 \text{ mA h g}^{-1}$  at  $100 \text{ mA g}^{-1}$  (100 cycles),  $332.4 \text{ mA h g}^{-1}$  at  $500 \text{ mA g}^{-1}$  (1000 cycles) and  $319 \text{ mA h g}^{-1}$  at  $1000 \text{ mA g}^{-1}$  after 5000 cycles (see Figure 5a–c). The authors suggested that the excellent physicochemical properties of Biochar-1 such as high percent of mesopores, more ordered graphitic structure and the presence of nitrogen groups in its structure yielded much better electrochemical performances when compared to disordered KOH activated biochar-2. Nathan A. Banek et al. [78] produced biochar materials from dried chlorella (spherical) algae and interconnected it with Gr (BCG) with controllable morphologies for LIBs. The materials were tested as anodes for LIB that delivered a specific capacity of  $357 \text{ mA h g}^{-1}$  for 100 cycles (Figure 5d,e). Kaifeng Yu et al. [79] reported using wheat straw cellulose as a precursor for carbon material. When it tested as anode materials, it delivered an irreversible capacity of  $1420 \text{ mA h g}^{-1}$  with a current rate of 0.2 C after 100 cycles. At a high current rate of 5 C, the anode could deliver close to  $1000 \text{ mA h g}^{-1}$ .

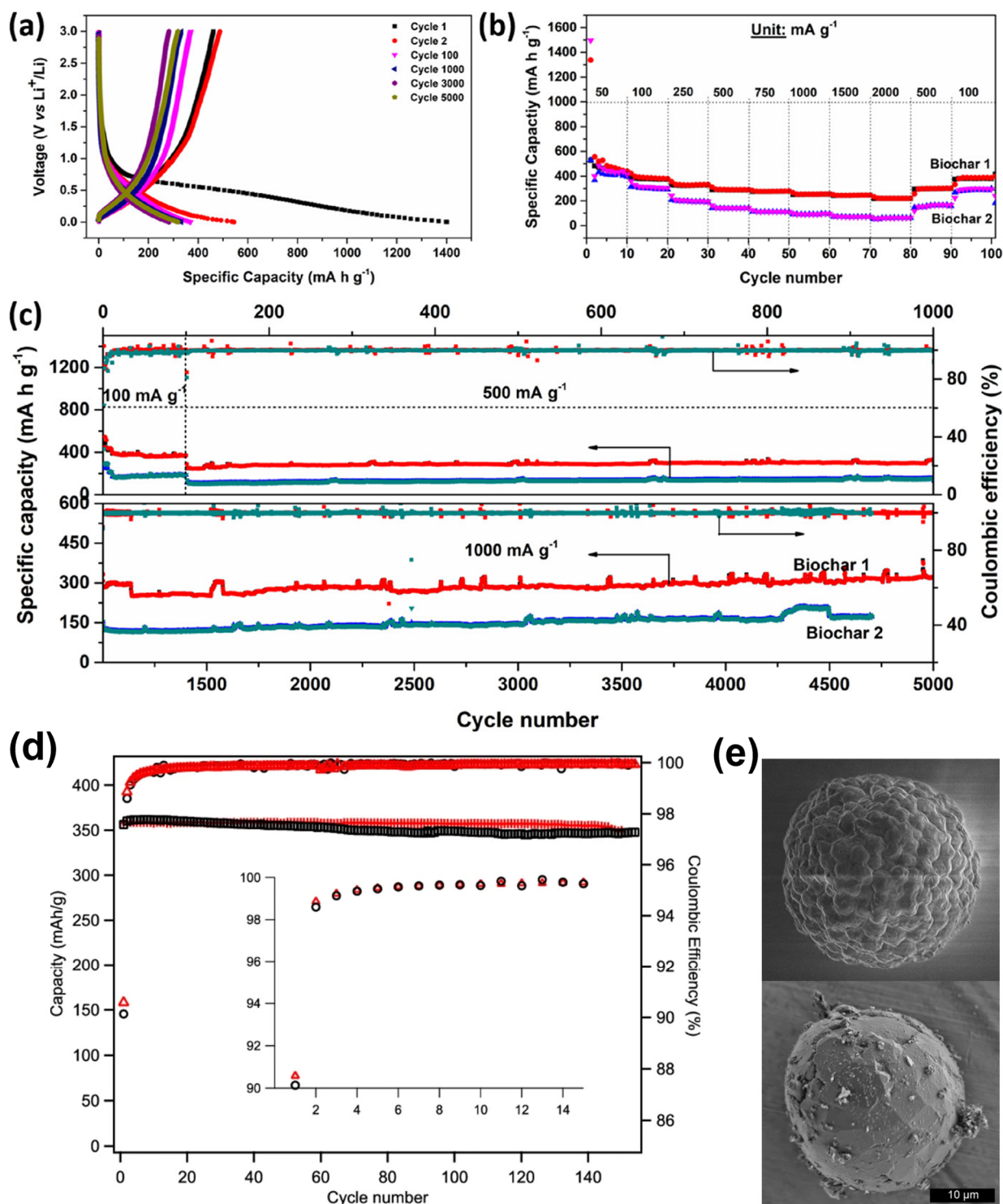


**Figure 5.** (a) Charge-discharge of biochar –1 at various cycles; (b) rate capability and (c) long-cycling profiles of biochars at different current densities. Reproduced from [77] with permission from ACS. (d) The electrochemical performances of biomass carbon sBCG and  $\text{MagE}_3$  (first 15 cycles of CE insect plots). (e) The morphology of raw spherical algae and BCG. The BCG is interconnected graphite flakes. Reproduced from [78] with permission from Springer Nature.

**Table 1.** Comparative electrochemical performance of biomass-based carbon material anodes for LIBs.

Biomass Source	Synthesis Method	Morphology	Specific Surface Area (SSA, m <sup>2</sup> /g)	Initial Capacity (Discharge/CHARGE) (mA h g <sup>-1</sup> )	Capacity Retention (mA h g <sup>-1</sup> )/(Cycles)	Rate Test (mA g <sup>-1</sup> ), (Cycle)/Capacity (mA h g <sup>-1</sup> )	Ref.
Sisal fiber	Hydrothermal activation method	Honeycomb (disordered carbon layers and micropores)	616.4	646	~550 (30)	-	[74]
Banana peel	high-temperature KOH activation method	High dense banana peel pseudo graphite	217	~2150/1075	800 (300)	10,000 (10) ~100	[80]
Bagasse	Hydrothermal activation method	N, P co-doped bagasse-based sheet-like mesoporous carbon	1307.21–2118.59	2347.56/1186.59	816.36 (50)	2000 (200) 592.38	[81]
Portobello mushroom	binder-free, and current collector-free Li-ion battery anodes	Carbon nanoribbon as free-standing	19.6	771.3/280	~260 (700)	-	[82]
Mustard seed waste	Hydrothermal method	high porous spherical carbon nanostructures in-situ doped of heteroatoms (N, S)	618	~822/617	~714 (550)	500 (10) 280	[83]
Tamarind plant Seeds	High temperature KOH activation method	porous carbon	103.51	~1037/414	~370 (100)	-	[84]
Rice Straws	high temperature KOH activation method	High porous carbon	3315	2041/986	-	744 (5) 257	[85]
Cherry Pit	KOH and H <sub>3</sub> PO <sub>4</sub> activation,	Disordered carbons	1662	~1300/300	200 (200)	1860 (5) 70	[75]
Jute Fiber	High temperature carbonization in open atmosphere	Micro-mesoporous carbon	1028.614	1173.3/534.1	427.2 (100)	1860 (10) 171.6	[86]
Coffee waste grounds	mechanochemical dry milling of spent coffee grounds followed by further carbonization at 800 °C	Non-porous carbonaceous materials	<10	764/~380	285 ± 5 (100)	1000 (10) 150	[87]
Spruce wood	pyrolysis and ball milling method	Spruce hard carbon	61	~400/250	300 (400)	1488 (10) ~110	[88]
Gold beard grass pollen	pyrolysis and KOH activation method	Mesoporous carbon powder from bee-collected pollens	1107.447	788.99	297.283 (200) @ 2000	5000 (-) 334.10	[89]

## 6. Biomass-Derived Carbon Anode for NIBs

Since the commercialization of LIBs, significant amounts of carbonaceous materials have been highly recognized as an anode because they have high surface areas. In particular, one of the carbonaceous materials Gr acts as a host for Li-ions because the high degree of structural ordering with interlayer distance is 3.35 Å. When 0.76 Å the ionic radius of lithium-ion is inserted into the Gr layer, its volume expansion could be observed at about 10.4%. The theoretical specific capacity for LiC<sub>6</sub> is 372 mA h g<sup>-1</sup>. This Gr is not suitable for the NIB anode. For understanding the limitations properly, the properties of the carbonaceous materials should be discussed. Normally, the Gr is a crystalline form of carbon (ordered) with a well-defined diffraction peak in the plane (002), and it is a good electron conductor. It also reacts with electrolytes forming the SEI layer. The stable SEI is helpful to maintain the cell more stable during cycling. While implementing the same Gr in NIB exhibits a very poor specific capacity of 35 mA h g<sup>-1</sup>. Considering that the specific capacity of K<sup>+</sup> with Gr is 279 mA h g<sup>-1</sup> and the Li, Na, and K ionic radius is 0.76, 1.86, and

2.27 Å respectively, a larger ionic radius is not only the cause of poor specific capacity. Then, what does hinder the intercalation process, especially for Na<sup>+</sup>? From the computational investigation [90], it was found that only negligible amounts of Na<sup>+</sup> contribute to the intercalation process due to the thermodynamic instability of intercalated Na<sup>+</sup>. During the intercalation process the as-mentioned alkali ion act as an electron donor concerning the Gr layer. Once it is stacked inside the layer, based on interaction with carbon molecules in the Gr layer, they form different compositions and crystalline phases. For example, LiC<sub>6</sub> or KC<sub>8</sub> in the case of Li and K respectively. Whereas, for sodium, low sodium content phases are found, for instance, NaC<sub>48</sub>, NaC<sub>64</sub>, and NaC<sub>80</sub> [91,92]. Compared to Li and K, Na has a higher stage index than Na. To increase the amount of Na in the graphite anode, other carbonaceous materials would be investigated. The better choice is hard carbon. The adjective “hard” refers to the reluctance of transforming from non-Gr to Gr form at elevated temperature. Therefore, it is named hard carbon (non-graphitizable carbon) and it can be identified using diffraction peaks broadness of the (002) reflection.

Gr-based materials, alloys, transition metal oxides, and other materials have been widely studied as promising anodes for NIBs. Among these materials, alloys, and transition metal oxides are suffering from poor electrochemical performance and larger volume expansion [17,92]. Therefore, biomass-derived carbon materials are the most suitable materials for practical application and attracted as a low-cost and more resource-abundant, high conductivity, and environmentally friendly material and possess high electrochemical performances when employed in NIBs. Still, hard carbon limits the practical applications for NIBs, due to the poor cycling stability. Gejun Shi, et al. [93] used cocklebur fruit as biomass to intercalate with N/O co-doped hard carbon via the pyrolysis heat treatment method. The highest synthesized temperature 1100 °C (H1100) of biomass anode delivers an excellent capacity of 366.07 mA h g<sup>-1</sup> with 69.08% ICE. From this approach, the N/O groups and Gr stabilizes and enable the high energy density of NIBs (Figure 6a,b). Hai-Yan Hu et al. [10] reported using waste bagasse biomass as a carbon source to produce hard carbon anodes by high-temperature thermal decomposition using various processing temperatures (900, 1000, and 1100 °C). This anode promises long-term stability of 91.5% capacity retention over 800 cycles with a current rate of 1000 mA g<sup>-1</sup>. Tested as a full cell having O<sub>3</sub>-type Na[Li<sub>0.05</sub>Ni<sub>0.3</sub>Mn<sub>0.5</sub>Cu<sub>0.1</sub>Mg<sub>0.05</sub>]O<sub>2</sub> as a cathode, the hard carbon anode delivered a high specific capacity of 112.2 mA h g<sup>-1</sup> at the current rate of 0.1 C and voltage range of 1.9–3.9 V (Figure 6c,d). Table 2 represents an overview of biomass precursors, methods for processing biomass, morphology, and electrochemical performance of NIBs for the recent research progress.

**Table 2.** Comparative electrochemical performance of biomass-based carbon material anodes for NIBs.

Biomass Source	Synthesis Method	Morphology	Specific Surface Area (SSA, m <sup>2</sup> /g)	Initial Capacity (Dis-charge/CHARGE) (mA h g <sup>-1</sup> )	Capacity Retention (mA h g <sup>-1</sup> )/(Cycles)/Current Rate (mA g <sup>-1</sup> )	Rate Test (mA g <sup>-1</sup> ), (Cycle)/Capacity (mA h g <sup>-1</sup> )	Ref.
bagasse-derived hard carbon	facile high temperature thermal decomposition method	sheet structure (HC 1000)	92.3	242.1/331.3	~100 (1000)/1000	25 (5)~331	[10]
camphor wood residues	carbonization followed by pyrolysis method	porous morphology	3.74	~324.6/391.8	268.1 (200)/20	20 (50)~319	[94]
Tea tomentia	High temperature treatment method	rod like morphology	13.92	~326.1	~262.4 (100)/28	-	[95]
cucumber stem	carbonization followed by KOH activation method	-	1988.90	~1200/458.6	198.6 (500)/50	-	[96]

Table 2. Cont.

Biomass Source	Synthesis Method	Morphology	Specific Surface Area (SSA, m <sup>2</sup> /g)	Initial Capacity (Discharge/CHARGE) (mA h g <sup>-1</sup> )	Capacity Retention (mA h g <sup>-1</sup> )/(Cycles)/Current Rate (mA g <sup>-1</sup> )	Rate Test (mA g <sup>-1</sup> ), (Cycle)/Capacity (mA h g <sup>-1</sup> )	Ref.
chickpea husk	sonochemical activation method,	honeycomb-like morphology	1599	~800/330	~125 (500)/20	1000 (500) 125	[97]
seaweed-derived carbon	High porous carbon by high temperature KOH activation method	sheet like carbon structure	1641	1342/287	192 (500)/100	800 (10) 114	[98]
Cotton roll	carbonization followed by pyrolysis method	braided fibrous morphology and hollow structure	38	~315	~262.4 (100)/30	-	[99]
drug residue	Heat treatment method	porous structure	989.7	~801/-	402 (500)/100	-	[100]

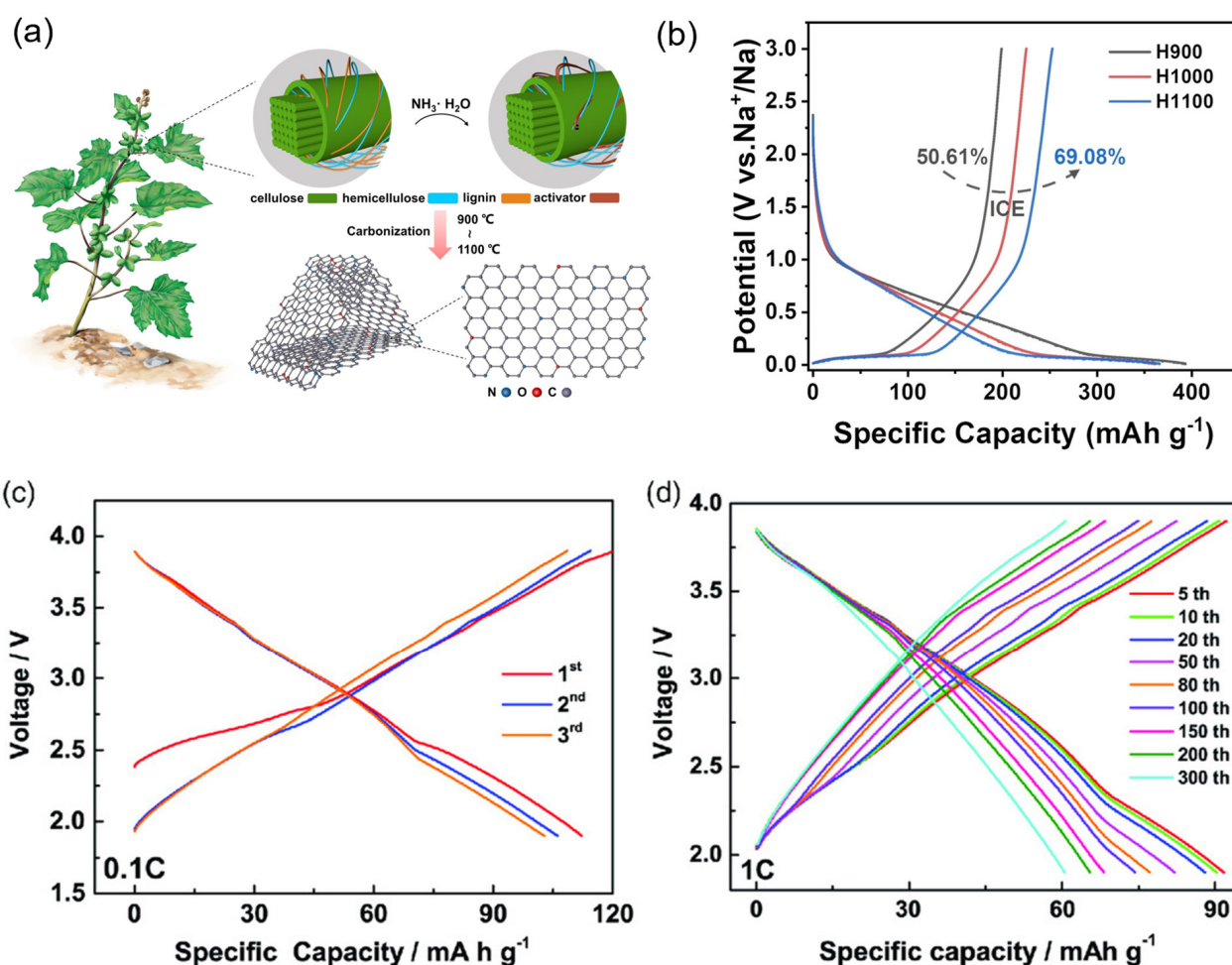


**Figure 6.** (a) The cocklebur fruit used as a biomass and synthesis of carbon anode materials for NIBs. (b) The electrochemical performance of first discharge and charge profiles for carbon materials with different synthesis temperatures (900, 1000, and 1100 °C). Reproduced from [93] with permission from Wiley. (c,d) The first three cycles of O<sub>3</sub>-Na[Li<sub>0.05</sub>Ni<sub>0.3</sub>Mn<sub>0.5</sub>Cu<sub>0.1</sub>Mg<sub>0.05</sub>]O<sub>2</sub> (NaLNMC) as a cathode and hard carbon biomass as an anode, with a rate of 0.1 C and cycling profiles versus specific capacity for the intermediate cycles with the constant current rate of 1 C. Reproduced from [10] with permission from Wiley.

## 7. Conclusions and Outlook

Given the need to develop more sustainable and greener battery systems, which also depends on materials availability and sustainable processing required for the batteries. To replace and/or compete with LIBs, NIBs are the most promising technology for large-scale energy storage systems. Huge efforts have been made to fabricate anode materials for high-performance LIBs and NIBs. Accordingly, this review addressed the employment of biomass resources to produce carbon anodes correlating their structures, pyrolysis behaviors, and controllable conversion with LIBs and NIBs energy storage applications.

Due to biomass natural abundance, sustainability, renewability, and morphological and structural variety, it has become an extremely suitable candidate for fabricating advanced anode materials for high-performance LIBs and NIBs. The employment of biomass carbon anode materials for LIBs and NIBs not only can speed up the development of greener energy storage technologies but also can effectively tackle the key issues regarding high-energy density, high safety, and low-cost devices. Therefore, designing a high-performance and fully bio-derived energy storage device is pretty much needed.

However, although all the advantages, some challenges remain as follows:

Insufficient knowledge on correlating the biomass characteristics/composition and biomass-derived carbon materials properties with desirable microstructures suitability for LIBs and NIBs applications.

Insufficient knowledge on controlling and tailoring the pore geometry and interlayer carbon spacing of the carbon materials, which are very important parameters for high-performance anode materials; for that the use of chemical activators and heteroatom dopants are suitable strategies, but their acting mechanisms are still unclear.

Biomass-derived materials ranging from inorganic multi-dimensional carbons can contribute to sustainable battery systems and components. This review also offers a comprehensive overview of the fabrication and application of biomass-derived materials in LIBs and NIBs. In more efficient and economical ways, battery materials may be available from biomass-derived materials. Anode materials are a prominent example of this kind of chemical and are investigated by many research groups for LIBs and NIBs applications. More attention should be paid to upgrading the processing technologies to maximize biomass-based materials utilization with high efficiency and low cost to accelerate upscaling and industrial applications. Overall, biomass-derived anode materials are most promising for LIBs and NIBs, especially considering the environmental impact arising from Gr extraction, which poses a huge problem across the world. In addition, the recent growth in the production of EVs and the consequent ever-increasing demand for LIBs and NIBs can drive industries to focus their attention on sustainable biomass anode materials.

**Author Contributions:** Conceptualization, P.M. and G.S.D.R.; investigation, P.M. and G.S.D.R.; writing—original draft preparation, P.M. and G.S.D.R.; writing—review and editing, D.K., C.M.S., U.L. and F.G.-A.; funding acquisition, U.L. and F.G.-A. All authors have read and agreed to the published version of the manuscript.

**Funding:** This research was funded by EU Interreg Nord/SolBat project, grant number 20202885.

**Institutional Review Board Statement:** Not applicable.

**Informed Consent Statement:** Not applicable.

**Data Availability Statement:** Not applicable.

**Acknowledgments:** Glaydson Simões Dos Reis thanks the Bio4Energy—a Strategic Research Environment appointed by the Swedish government and the Swedish University of Agricultural Sciences, for the funding support.

**Conflicts of Interest:** The authors declare no conflict of interest.

## References

1. Abdelbaky, M.; Peeters, J.R.; Dewulf, W. On the Influence of Second Use, Future Battery Technologies, and Battery Lifetime on the Maximum Recycled Content of Future Electric Vehicle Batteries in Europe. *Waste Manag.* **2021**, *125*, 1–9. [[CrossRef](#)] [[PubMed](#)]
2. Ding, Y.; Cano, Z.P.; Yu, A.; Lu, J.; Chen, Z. Automotive Li-Ion Batteries: Current Status and Future Perspectives. *Electrochem. Energy Rev.* **2019**, *2*, 1–28. [[CrossRef](#)]
3. Cavers, H.; Molaiyan, P.; Abdollahifar, M.; Lassi, U.; Kwade, A. Perspectives on Improving the Safety and Sustainability of High Voltage Lithium-Ion Batteries Through the Electrolyte and Separator Region. *Adv. Energy Mater.* **2022**, *12*, 2200147. [[CrossRef](#)]
4. Kim, T.; Song, W.; Son, D.-Y.; Ono, L.K.; Qi, Y. Lithium-Ion Batteries: Outlook on Present, Future, and Hybridized Technologies. *J. Mater. Chem. A* **2019**, *7*, 2942–2964. [[CrossRef](#)]
5. Tarascon, J.-M. Is Lithium the New Gold? *Nat. Chem.* **2010**, *2*, 510. [[CrossRef](#)]
6. Zhao, L.; Zhang, T.; Li, W.; Li, T.; Zhang, L.; Zhang, X.; Wang, Z. Engineering of Sodium-Ion Batteries: Opportunities and Challenges. *Engineering* **2022**. [[CrossRef](#)]
7. Mohan, I.; Raj, A.; Shubham, K.; Lata, D.B.; Mandal, S.; Kumar, S. Potential of Potassium and Sodium-Ion Batteries as the Future of Energy Storage: Recent Progress in Anodic Materials. *J. Energy Storage* **2022**, *55*, 105625. [[CrossRef](#)]
8. Tarascon, J.-M. Na-Ion versus Li-Ion Batteries: Complementarity Rather than Competitiveness. *Joule* **2020**, *4*, 1616–1620. [[CrossRef](#)]
9. Madian, M.; Eychmüller, A.; Giebeler, L. Current Advances in TiO<sub>2</sub>-Based Nanostructure Electrodes for High Performance Lithium Ion Batteries. *Batteries* **2018**, *4*, 7. [[CrossRef](#)]
10. Hu, H.-Y.; Xiao, Y.; Ling, W.; Wu, Y.-B.; Wang, P.; Tan, S.-J.; Xu, Y.-S.; Guo, Y.-J.; Chen, W.-P.; Tang, R.-R.; et al. A Stable Biomass-Derived Hard Carbon Anode for High-Performance Sodium-Ion Full Battery. *Energy Technol.* **2021**, *9*, 2000730. [[CrossRef](#)]
11. Zhang, H.; Yang, Y.; Ren, D.; Wang, L.; He, X. Graphite as Anode Materials: Fundamental Mechanism, Recent Progress and Advances. *Energy Storage Mater.* **2021**, *36*, 147–170. [[CrossRef](#)]
12. Agubra, V.A.; Fergus, J.W. The Formation and Stability of the Solid Electrolyte Interface on the Graphite Anode. *J. Power Sources* **2014**, *268*, 153–162. [[CrossRef](#)]
13. Abdollahifar, M.; Molaiyan, P.; Lassi, U.; Wu, N.L.; Kwade, A. Multifunctional Behaviour of Graphite in Lithium–Sulfur Batteries. *Renew. Sustain. Energy Rev.* **2022**, *169*, 112948. [[CrossRef](#)]
14. Wang, W.; Ruiz, I.; Guo, S.; Favors, Z.; Bay, H.H.; Ozkan, M.; Ozkan, C.S. Hybrid Carbon Nanotube and Graphene Nanostructures for Lithium Ion Battery Anodes. *Nano Energy* **2014**, *3*, 113–118. [[CrossRef](#)]
15. Ren, J.; Ren, R.-P.; Lv, Y.-K. A New Anode for Lithium-Ion Batteries Based on Single-Walled Carbon Nanotubes and Graphene: Improved Performance through a Binary Network Design. *Chem. Asian J.* **2018**, *13*, 1223–1227. [[CrossRef](#)]
16. Saifuddin, N.; Raziah, A.Z.; Junizah, A.R. Carbon Nanotubes: A Review on Structure and Their Interaction with Proteins. *J. Chem.* **2013**, *2013*, 676815. [[CrossRef](#)]
17. Abdollahifar, M.; Molaiyan, P.; Perovic, M.; Kwade, A. Insights into Enhancing Electrochemical Performance of Li-Ion Battery Anodes via Polymer Coating. *Energies* **2022**, *15*, 8791. [[CrossRef](#)]
18. Liu, A.; Liu, T.-F.; Yuan, H.-D.; Wang, Y.; Liu, Y.-J.; Luo, J.-M.; Nai, J.-W.; Tao, X.-Y. A Review of Biomass-Derived Carbon Materials for Lithium Metal Anodes. *New Carbon Mater.* **2022**, *37*, 658–674. [[CrossRef](#)]
19. Alvira, D.; Antorán, D.; Manyà, J.J. Plant-Derived Hard Carbon as Anode for Sodium-Ion Batteries: A Comprehensive Review to Guide Interdisciplinary Research. *Chem. Eng. J.* **2022**, *447*, 137468. [[CrossRef](#)]
20. dos Reis, G.S.; Pinheiro Lima, R.M.A.; Larsson, S.H.; Subramaniam, C.M.; Dinh, V.M.; Thyrel, M.; de Oliveira, H.P. Flexible Supercapacitors of Biomass-Based Activated Carbon-Polypyrrole on Eggshell Membranes. *J. Environ. Chem. Eng.* **2021**, *9*, 106155. [[CrossRef](#)]
21. Reis, G.S.; Oliveira, H.P.; Larsson, S.H.; Thyrel, M.; Claudio Lima, E. A Short Review on the Electrochemical Performance of Hierarchical and Nitrogen-Doped Activated Biocarbon-Based Electrodes for Supercapacitors. *Nanomaterials* **2021**, *11*, 424. [[CrossRef](#)]
22. Dos Reis, G.S.; Larsson, S.H.; de Oliveira, H.P.; Thyrel, M.; Lima, E.C. Sustainable Biomass Activated Carbons as Electrodes for Battery and Supercapacitors—A Mini-Review. *Nanomaterials* **2020**, *10*, 1398. [[CrossRef](#)] [[PubMed](#)]
23. Yao, Y.; Wu, F. Naturally Derived Nanostructured Materials from Biomass for Rechargeable Lithium/Sodium Batteries. *Nano Energy* **2015**, *17*, 91–103. [[CrossRef](#)]
24. Wu, F.; Liu, L.; Yuan, Y.; Li, Y.; Bai, Y.; Li, T.; Lu, J.; Wu, C. Expanding Interlayer Spacing of Hard Carbon by Natural K<sup>+</sup> Doping to Boost Na-Ion Storage. *ACS Appl. Mater. Interfaces* **2018**, *10*, 27030–27038. [[CrossRef](#)]
25. González-Hourcade, M.; Simões dos Reis, G.; Grimm, A.; Dinh, V.M.; Lima, E.C.; Larsson, S.H.; Gentili, F.G. Microalgae Biomass as a Sustainable Precursor to Produce Nitrogen-Doped Biochar for Efficient Removal of Emerging Pollutants from Aqueous Media. *J. Clean. Prod.* **2022**, *348*, 131280. [[CrossRef](#)]
26. Deng, Q.; Liu, H.; Zhou, Y.; Luo, Z.; Wang, Y.; Zhao, Z.; Yang, R. N-Doped Three-Dimensional Porous Carbon Materials Derived from Bagasse Biomass as an Anode Material for K-Ion Batteries. *J. Electroanal. Chem.* **2021**, *899*, 115668. [[CrossRef](#)]
27. Sliz, R.; Molaiyan, P.; Fabritius, T.; Lassi, U. Printed Electronics to Accelerate Solid-State Battery Development. *Nano Express* **2022**, *3*, 021002. [[CrossRef](#)]
28. Li, M.; Lu, J.; Chen, Z.; Amine, K. 30 Years of Lithium-Ion Batteries. *Adv. Mater.* **2018**, *30*, 1800561. [[CrossRef](#)]
29. Manthiram, A. A Reflection on Lithium-Ion Battery Cathode Chemistry. *Nat. Commun.* **2020**, *11*, 1550. [[CrossRef](#)] [[PubMed](#)]

30. Yao, Y.; Chen, Z.; Yu, R.; Chen, Q.; Zhu, J.; Hong, X.; Zhou, L.; Wu, J.; Mai, L. Confining Ultrafine MoO<sub>2</sub> in a Carbon Matrix Enables Hybrid Li Ion and Li Metal Storage. *ACS Appl. Mater. Interfaces* **2020**, *12*, 40648–40654. [[CrossRef](#)]
31. Subramaniam, C.M.; Islam, M.M.; Akhter, T.; Cardillo, D.; Konstantinov, K.; Liu, H.K.; Dou, S.X. A Chemically Modified Graphene Oxide Wrapped Porous Hematite Nano-Architecture as a High Rate Lithium-Ion Battery Anode Material. *RSC Adv.* **2016**, *6*, 82698–82706. [[CrossRef](#)]
32. Poizot, P.; Laruelle, S.; Grugeon, S.; Dupont, L.; Tarascon, J.-M. Nano-Sized Transition-Metal Oxides as Negative-Electrode Materials for Lithium-Ion Batteries. *Nature* **2000**, *407*, 496–499. [[CrossRef](#)] [[PubMed](#)]
33. Peters, J.F.; Peña Cruz, A.; Weil, M. Exploring the Economic Potential of Sodium-Ion Batteries. *Batteries* **2019**, *5*, 10. [[CrossRef](#)]
34. Pu, X.; Wang, H.; Zhao, D.; Yang, H.; Ai, X.; Cao, S.; Chen, Z.; Cao, Y. Recent Progress in Rechargeable Sodium-Ion Batteries: Toward High-Power Applications. *Small* **2019**, *15*, 1805427. [[CrossRef](#)] [[PubMed](#)]
35. Li, Q.; Yu, X.; Li, H. Batteries: From China's 13th to 14th Five-Year Plan. *eTransportation* **2022**, *14*, 100201. [[CrossRef](#)]
36. Yabuuchi, N.; Kajiyama, M.; Iwatate, J.; Nishikawa, H.; Hitomi, S.; Okuyama, R.; Usui, R.; Yamada, Y.; Komaba, S. P2-Type Na<sub>x</sub>[Fe<sup>1/2</sup>Mn<sup>1/2</sup>]O<sub>2</sub> Made from Earth-Abundant Elements for Rechargeable Na Batteries. *Nat. Mater.* **2012**, *11*, 512–517. [[CrossRef](#)]
37. Shi, Y.; Feng, Y.; Zhang, Q.; Shuai, J.; Niu, J. Does China's New Energy Vehicles Supply Chain Stock Market Have Risk Spillovers? Evidence from Raw Material Price Effect on Lithium Batteries. *Energy* **2023**, *262*, 125420. [[CrossRef](#)]
38. Keller, M.; Buchholz, D.; Passerini, S. Layered Na-Ion Cathodes with Outstanding Performance Resulting from the Synergetic Effect of Mixed P- and O-Type Phases. *Adv. Energy Mater.* **2016**, *6*, 1501555. [[CrossRef](#)]
39. Xie, F.; Xu, Z.; Guo, Z.; Titirici, M.-M. Hard Carbons for Sodium-Ion Batteries and Beyond. *Prog. Energy* **2020**, *2*, 42002. [[CrossRef](#)]
40. Chang, Y.-M.; Lin, H.-W.; Li, L.-J.; Chen, H.-Y. Two-Dimensional Materials as Anodes for Sodium-Ion Batteries. *Mater. Today Adv.* **2020**, *6*, 100054. [[CrossRef](#)]
41. Hirsh, H.S.; Li, Y.; Tan, D.H.S.; Zhang, M.; Zhao, E.; Meng, Y.S. Sodium-Ion Batteries Paving the Way for Grid Energy Storage. *Adv. Energy Mater.* **2020**, *10*, 2001274. [[CrossRef](#)]
42. Darga, J.; Lamb, J.; Manthiram, A. Industrialization of Layered Oxide Cathodes for Lithium-Ion and Sodium-Ion Batteries: A Comparative Perspective. *Energy Technol.* **2020**, *8*, 2000723. [[CrossRef](#)]
43. Barpanda, P.; Oyama, G.; Nishimura, S.I.; Chung, S.C.; Yamada, A. A 3.8-V Earth-Abundant Sodium Battery Electrode. *Nat. Commun.* **2014**, *5*, 4358. [[CrossRef](#)] [[PubMed](#)]
44. Slater, M.D.; Kim, D.; Lee, E.; Johnson, C.S. Sodium-Ion Batteries. *Adv. Funct. Mater.* **2013**, *23*, 947–958. [[CrossRef](#)]
45. Iqbal, S.; Khatoun, H.; Hussain Pandit, A.; Ahmad, S. Recent Development of Carbon Based Materials for Energy Storage Devices. *Mater. Sci. Energy Technol.* **2019**, *2*, 417–428. [[CrossRef](#)]
46. Franklin, R.E.; Randall, J.T. Crystallite Growth in Graphitizing and Non-Graphitizing Carbons. *Proc. R. Soc. London. Ser. A. Math. Phys. Sci.* **1951**, *209*, 196–218. [[CrossRef](#)]
47. Huang, S.; Li, Z.; Wang, B.; Zhang, J.; Peng, Z.; Qi, R.; Wang, J.; Zhao, Y. N-Doping and Defective Nanographitic Domain Coupled Hard Carbon Nanoshells for High Performance Lithium/Sodium Storage. *Adv. Funct. Mater.* **2018**, *28*, 1706294. [[CrossRef](#)]
48. Tian, W.; Wang, L.; Huo, K.; He, X. Red Phosphorus Filled Biomass Carbon as High-Capacity and Long-Life Anode for Sodium-Ion Batteries. *J. Power Sources* **2019**, *430*, 60–66. [[CrossRef](#)]
49. Guizani, C.; Jeguirim, M.; Valin, S.; Limousy, L.; Salvador, S. Biomass Chars: The Effects of Pyrolysis Conditions on Their Morphology, Structure, Chemical Properties and Reactivity. *Energies* **2017**, *10*, 796. [[CrossRef](#)]
50. Jerigová, M.; Odziomek, M.; López-Salas, N. "We Are Here!" Oxygen Functional Groups in Carbons for Electrochemical Applications. *ACS Omega* **2022**, *7*, 11544–11554. [[CrossRef](#)]
51. Zhao, H.; Ye, J.; Song, W.; Zhao, D.; Kang, M.; Shen, H.; Li, Z. Insights into the Surface Oxygen Functional Group-Driven Fast and Stable Sodium Adsorption on Carbon. *ACS Appl. Mater. Interfaces* **2020**, *12*, 6991–7000. [[CrossRef](#)]
52. Sun, F.; Wang, H.; Qu, Z.; Wang, K.; Wang, L.; Gao, J.; Gao, J.; Liu, S.; Lu, Y. Carboxyl-Dominant Oxygen Rich Carbon for Improved Sodium Ion Storage: Synergistic Enhancement of Adsorption and Intercalation Mechanisms. *Adv. Energy Mater.* **2021**, *11*, 2002981. [[CrossRef](#)]
53. Wang, L.; Zhuo, L.; Cheng, H.; Zhang, C.; Zhao, F. Porous Carbon Nanotubes Decorated with Nanosized Cobalt Ferrite as Anode Materials for High-Performance Lithium-Ion Batteries. *J. Power Sources* **2015**, *283*, 289–299. [[CrossRef](#)]
54. Collins, J.; Gourdin, G.; Foster, M.; Qu, D. Carbon Surface Functionalities and SEI Formation during Li Intercalation. *Carbon N. Y.* **2015**, *92*, 193–244. [[CrossRef](#)]
55. Ventosa, E.; Xia, W.; Klink, S.; La Mantia, F.; Muhler, M.; Schuhmann, W. Influence of Surface Functional Groups on Lithium Ion Intercalation of Carbon Cloth. *Electrochim. Acta* **2012**, *65*, 22–29. [[CrossRef](#)]
56. Saha, N.; Xin, D.; Chiu, P.C.; Reza, M.T. Effect of Pyrolysis Temperature on Acidic Oxygen-Containing Functional Groups and Electron Storage Capacities of Pyrolyzed Hydrochars. *ACS Sustain. Chem. Eng.* **2019**, *7*, 8387–8396. [[CrossRef](#)]
57. Chen, W.; Wan, M.; Liu, Q.; Xiong, X.; Yu, F.; Huang, Y. Heteroatom-Doped Carbon Materials: Synthesis, Mechanism, and Application for Sodium-Ion Batteries. *Small Methods* **2019**, *3*, 1800323. [[CrossRef](#)]
58. Soo, L.T.; Loh, K.S.; Mohamad, A.B.; Daud, W.R.W.; Wong, W.Y. Effect of Nitrogen Precursors on the Electrochemical Performance of Nitrogen-Doped Reduced Graphene Oxide towards Oxygen Reduction Reaction. *J. Alloys Compd.* **2016**, *677*, 112–120. [[CrossRef](#)]
59. Sánchez-González, J.; Stoeckli, F.; Centeno, T.A. The Role of the Electric Conductivity of Carbons in the Electrochemical Capacitor Performance. *J. Electroanal. Chem.* **2011**, *657*, 176–180. [[CrossRef](#)]

60. Chandra, S.; Bhattacharya, J. Influence of Temperature and Duration of Pyrolysis on the Property Heterogeneity of Rice Straw Biochar and Optimization of Pyrolysis Conditions for Its Application in Soils. *J. Clean. Prod.* **2019**, *215*, 1123–1139. [[CrossRef](#)]
61. Wang, Y.; Santiago-Aviles, J.J.; Furlan, R.; Ramos, I. Pyrolysis Temperature and Time Dependence of Electrical Conductivity Evolution for Electrostatically Generated Carbon Nanofibers. *IEEE Trans. Nanotechnol.* **2003**, *2*, 39–43. [[CrossRef](#)]
62. Barroso-Bogeat, A.; Alexandre-Franco, M.; Fernández-González, C.; Macías-García, A.; Gómez-Serrano, V. Temperature Dependence of the Electrical Conductivity of Activated Carbons Prepared from Vine Shoots by Physical and Chemical Activation Methods. *Microporous Mesoporous Mater.* **2015**, *209*, 90–98. [[CrossRef](#)]
63. Konikkara, N.; Kennedy, L.J.; Aruldoss, U.; Vijaya, J.J. Electrical Conductivity Studies of Nanoporous Carbon Derived from Leather Waste: Effect of Pressure, Temperature and Porosity. *J. Nanosci. Nanotechnol.* **2016**, *16*, 8829–8838. [[CrossRef](#)]
64. Mousavi, H.; Moradian, R. Nitrogen and Boron Doping Effects on the Electrical Conductivity of Graphene and Nanotube. *Solid State Sci.* **2011**, *13*, 1459–1464. [[CrossRef](#)]
65. Qiao, M.; Tang, C.; He, G.; Qiu, K.; Binions, R.; Parkin, I.P.; Zhang, Q.; Guo, Z.; Titirici, M.M. Graphene/Nitrogen-Doped Porous Carbon Sandwiches for the Metal-Free Oxygen Reduction Reaction: Conductivity versus Active Sites. *J. Mater. Chem. A* **2016**, *4*, 12658–12666. [[CrossRef](#)]
66. Jin, Q.; Li, W.; Wang, K.; Feng, P.; Li, H.; Gu, T.; Zhou, M.; Wang, W.; Cheng, S.; Jiang, K. Experimental Design and Theoretical Calculation for Sulfur-Doped Carbon Nanofibers as a High Performance Sodium-Ion Battery Anode. *J. Mater. Chem. A* **2019**, *7*, 10239–10245. [[CrossRef](#)]
67. Zhang, Y.; Chen, L.; Meng, Y.; Li, X.; Guo, Y.; Xiao, D. Sodium Storage in Fluorine-Rich Mesoporous Carbon Fabricated by Low-Temperature Carbonization of Polyvinylidene Fluoride with a Silica Template. *RSC Adv.* **2016**, *6*, 110850–110857. [[CrossRef](#)]
68. Nakajima, T.; Gupta, V.; Ohzawa, Y.; Koh, M.; Singh, R.N.; Tressaud, A.; Durand, E. Electrochemical Behavior of Plasma-Fluorinated Graphite for Lithium Ion Batteries. *J. Power Sources* **2002**, *104*, 108–114. [[CrossRef](#)]
69. Guy, M.; Mathieu, M.; Anastopoulos, I.P.; Martínez, M.G.; Rousseau, F.; Dotto, G.L.; de Oliveira, H.P.; Lima, E.C.; Thyrel, M.; Larsson, S.H.; et al. Process Parameters Optimization, Characterization, and Application of KOH-Activated Norway Spruce Bark Graphitic Biochars for Efficient Azo Dye Adsorption. *Molecules* **2022**, *27*, 456. [[CrossRef](#)]
70. Bouchelta, C.; Medjram, M.S.; Zoubida, M.; Chekkat, F.A.; Ramdane, N.; Bellat, J.-P. Effects of Pyrolysis Conditions on the Porous Structure Development of Date Pits Activated Carbon. *J. Anal. Appl. Pyrolysis* **2012**, *94*, 215–222. [[CrossRef](#)]
71. Ahmad, M.; Lee, S.S.; Dou, X.; Mohan, D.; Sung, J.-K.; Yang, J.E.; Ok, Y.S. Effects of Pyrolysis Temperature on Soybean Stover- and Peanut Shell-Derived Biochar Properties and TCE Adsorption in Water. *Bioresour. Technol.* **2012**, *118*, 536–544. [[CrossRef](#)]
72. dos Reis, G.S.; Larsson, S.H.; Thyrel, M.; Pham, T.N.; Claudio Lima, E.; de Oliveira, H.P.; Dotto, G.L. Preparation and Application of Efficient Biobased Carbon Adsorbents Prepared from Spruce Bark Residues for Efficient Removal of Reactive Dyes and Colors from Synthetic Effluents. *Coatings* **2021**, *11*, 772. [[CrossRef](#)]
73. dos Reis, G.S.; Guy, M.; Mathieu, M.; Jebrane, M.; Lima, E.C.; Thyrel, M.; Dotto, G.L.; Larsson, S.H. A Comparative Study of Chemical Treatment by  $MgCl_2$ ,  $ZnSO_4$ ,  $ZnCl_2$ , and KOH on Physicochemical Properties and Acetaminophen Adsorption Performance of Biobased Porous Materials from Tree Bark Residues. *Colloids Surf. A Physicochem. Eng. Asp.* **2022**, *642*, 128626. [[CrossRef](#)]
74. Yu, X.; Zhang, K.; Tian, N.; Qin, A.; Liao, L.; Du, R.; Wei, C. Biomass Carbon Derived from Sisal Fiber as Anode Material for Lithium-Ion Batteries. *Mater. Lett.* **2015**, *142*, 193–196. [[CrossRef](#)]
75. Hernández-Rentero, C.; Marangon, V.; Olivares-Marín, M.; Gómez-Serrano, V.; Caballero, Á.; Morales, J.; Hassoun, J. Alternative Lithium-Ion Battery Using Biomass-Derived Carbons as Environmentally Sustainable Anode. *J. Colloid Interface Sci.* **2020**, *573*, 396–408. [[CrossRef](#)] [[PubMed](#)]
76. Dou, Y.; Liu, X.; Yu, K.; Wang, X.; Liu, W.; Liang, J.; Liang, C. Biomass Porous Carbon Derived from Jute Fiber as Anode Materials for Lithium-Ion Batteries. *Diam. Relat. Mater.* **2019**, *98*, 107514. [[CrossRef](#)]
77. dos Reis, S.G.; Mayandi Subramaniam, C.; Cárdenas, A.D.; Larsson, S.H.; Thyrel, M.; Lassi, U.; García-Alvarado, F. Facile Synthesis of Sustainable Activated Biochars with Different Pore Structures as Efficient Additive-Carbon-Free Anodes for Lithium- and Sodium-Ion Batteries. *ACS Omega* **2022**, *7*, 42570–42581. [[CrossRef](#)]
78. Banek, N.A.; McKenzie, K.R.; Abele, D.T.; Wagner, M.J. Sustainable Conversion of Biomass to Rationally Designed Lithium-Ion Battery Graphite. *Sci. Rep.* **2022**, *12*, 8080. [[CrossRef](#)]
79. Yu, K.; Wang, B.; Bai, P.; Liang, C.; Jin, W. Wheat Straw Cellulose Amorphous Porous Carbon Used as Anode Material for a Lithium-Ion Battery. *J. Electron. Mater.* **2021**, *50*, 6438–6447. [[CrossRef](#)]
80. Lotfabad, E.M.; Ding, J.; Cui, K.; Kohandehghan, A.; Kalisvaart, W.P.; Hazelton, M.; Mitlin, D. High-Density Sodium and Lithium Ion Battery Anodes from Banana Peels. *ACS Nano* **2014**, *8*, 7115–7129. [[CrossRef](#)]
81. Zheng, S.; Luo, Y.; Zhang, K.; Liu, H.; Hu, G.; Qin, A. Nitrogen and Phosphorus Co-Doped Mesoporous Carbon Nanosheets Derived from Bagasse for Lithium-Ion Batteries. *Mater. Lett.* **2021**, *290*, 129459. [[CrossRef](#)]
82. Campbell, B.; Ionescu, R.; Favors, Z.; Ozkan, C.S.; Ozkan, M. Bio-Derived, Binderless, Hierarchically Porous Carbon Anodes for Li-Ion Batteries. *Sci. Rep.* **2015**, *5*, 14575. [[CrossRef](#)]
83. Pramanik, A.; Chattopadhyay, S.; De, G.; Mahanty, S. Efficient Energy Storage in Mustard Husk Derived Porous Spherical Carbon Nanostructures. *Mater. Adv.* **2021**, *2*, 7463–7472. [[CrossRef](#)]

84. Panda, M.R.; Kathribail, A.R.; Modak, B.; Sau, S.; Dutta, D.P.; Mitra, S. Electrochemical Properties of Biomass-Derived Carbon and Its Composite along with Na<sub>2</sub>Ti<sub>3</sub>O<sub>7</sub> as Potential High-Performance Anodes for Na-Ion and Li-Ion Batteries. *Electrochim. Acta* **2021**, *392*, 139026. [[CrossRef](#)]
85. Zhang, F.; Wang, K.X.; Li, G.D.; Chen, J.S. Hierarchical Porous Carbon Derived from Rice Straw for Lithium Ion Batteries with High-Rate Performance. *Electrochem. Commun.* **2009**, *11*, 130–133. [[CrossRef](#)]
86. Dou, Y.; Liu, X.; Wang, X.; Yu, K.; Liang, C. Jute Fiber Based Micro-Mesoporous Carbon: A Biomass Derived Anode Material with High-Performance for Lithium-Ion Batteries. *Mater. Sci. Eng. B Solid-State Mater. Adv. Technol.* **2021**, *265*, 115015. [[CrossRef](#)]
87. Luna-Lama, F.; Rodríguez-Padrón, D.; Puente-Santiago, A.R.; Muñoz-Batista, M.J.; Caballero, A.; Balu, A.M.; Romero, A.A.; Luque, R. Non-Porous Carbonaceous Materials Derived from Coffee Waste Grounds as Highly Sustainable Anodes for Lithium-Ion Batteries. *J. Clean. Prod.* **2019**, *207*, 411–417. [[CrossRef](#)]
88. Drews, M.; Büttner, J.; Bauer, M.; Ahmed, J.; Sahu, R.; Scheu, C.; Vierrath, S.; Fischer, A.; Biro, D. Spruce Hard Carbon Anodes for Lithium-Ion Batteries. *ChemElectroChem* **2021**, *8*, 4750–4761. [[CrossRef](#)]
89. Kietisirirojana, N.; Tunkasiri, T.; Pengpat, K.; Khamman, O.; Intatha, U.; Eitssayeam, S. Synthesis of Mesoporous Carbon Powder from Gold Beard Grass Pollen for Use as an Anode for Lithium-Ion Batteries. *Microporous Mesoporous Mater.* **2022**, *331*, 111565. [[CrossRef](#)]
90. Moriwake, H.; Kuwabara, A.; Fisher, C.A.J.; Ikuhara, Y. Why Is Sodium-Intercalated Graphite Unstable? *RSC Adv.* **2017**, *7*, 36550–36554. [[CrossRef](#)]
91. Xu, Z.-L.; Yoon, G.; Park, K.-Y.; Park, H.; Tamwattana, O.; Joo Kim, S.; Seong, W.M.; Kang, K. Tailoring Sodium Intercalation in Graphite for High Energy and Power Sodium Ion Batteries. *Nat. Commun.* **2019**, *10*, 2598. [[CrossRef](#)]
92. Xu, Z.-L.; Park, J.; Yoon, G.; Kim, H.; Kang, K. Graphitic Carbon Materials for Advanced Sodium-Ion Batteries. *Small Methods* **2019**, *3*, 1800227. [[CrossRef](#)]
93. Shi, G.; Han, Z.; Hu, L.; Wang, B.; Huang, F. N/O Co-Doped Hard Carbon Derived from Cocklebur Fruit for Sodium-Ion Storage. *ChemElectroChem* **2022**, *9*, e202200138. [[CrossRef](#)]
94. Guo, S.; Chen, Y.; Tong, L.; Cao, Y.; Jiao, H.; Long, Z.; Qiu, X. Biomass Hard Carbon of High Initial Coulombic Efficiency for Sodium-Ion Batteries: Preparation and Application. *Electrochim. Acta* **2022**, *410*, 140017. [[CrossRef](#)]
95. Wang, H.; Chen, H.; Chen, C.; Li, M.; Xie, Y.; Zhang, X.; Wu, X.; Zhang, Q.; Lu, C. Tea-Derived Carbon Materials as Anode for High-Performance Sodium Ion Batteries. *Chin. Chem. Lett.* **2022**, *in press*. [[CrossRef](#)]
96. Li, C.; Li, J.; Zhang, Y.; Cui, X.; Lei, H.; Li, G. Heteroatom-Doped Hierarchically Porous Carbons Derived from Cucumber Stem as High-Performance Anodes for Sodium-Ion Batteries. *J. Mater. Sci.* **2019**, *54*, 5641–5657. [[CrossRef](#)]
97. Ghani, U.; Iqbal, N.; Aboalhassan, A.A.; Liu, B.; Aftab, T.; Zada, I.; Ullah, F.; Gu, J.; Li, Y.; Zhu, S.; et al. One-Step Sonochemical Fabrication of Biomass-Derived Porous Hard Carbons; towards Tuned-Surface Anodes of Sodium-Ion Batteries. *J. Colloid Interface Sci.* **2022**, *611*, 578–587. [[CrossRef](#)] [[PubMed](#)]
98. Senthil, C.; Park, J.W.; Shaji, N.; Sim, G.S.; Lee, C.W. Biomass Seaweed-Derived Nitrogen Self-Doped Porous Carbon Anodes for Sodium-Ion Batteries: Insights into the Structure and Electrochemical Activity. *J. Energy Chem.* **2021**, *64*, 286–295. [[CrossRef](#)]
99. Li, Y.; Hu, Y.S.; Titirici, M.M.; Chen, L.; Huang, X. Hard Carbon Microtubes Made from Renewable Cotton as High-Performance Anode Material for Sodium-Ion Batteries. *Adv. Energy Mater.* **2016**, *6*, 1600659. [[CrossRef](#)]
100. Wan, H.; Shen, X.; Jiang, H.; Zhang, C.; Jiang, K.; Chen, T.; Shi, L.; Dong, L.; He, C.; Xu, Y.; et al. Biomass-Derived N/S Dual-Doped Porous Hard-Carbon as High-Capacity Anodes for Lithium/Sodium Ions Batteries. *Energy* **2021**, *231*, 121102. [[CrossRef](#)]

**Disclaimer/Publisher’s Note:** The statements, opinions and data contained in all publications are solely those of the individual author(s) and contributor(s) and not of MDPI and/or the editor(s). MDPI and/or the editor(s) disclaim responsibility for any injury to people or property resulting from any ideas, methods, instructions or products referred to in the content.